Emergent Materials
https://doi.org/10.1007/s42247-025-01002-1

ORIGINAL ARTICLE

Development of natural sporopollenin microcapsules: from bee pollen to versatile biomaterials

Volkan Aylanc[1,2,3] · Seymanur Ertosun[1,2] · Andreia F. Peixoto[2] · Arantzazu Santamaria-Echart[1] · Paulo Russo-Almeida[4] · Nuno Vale[3,5,6] · Cristina Freire[2] · Miguel Vilas-Boas[1]

Received: 15 November 2024 / Accepted: 14 January 2025

Abstract

The outer layer of the pollen grain, which plays a crucial role in the continuity of terrestrial plant life, has received significant attention due to its robustness, chemical inertness, and biocompatible structure made of sporopollenin. Herein, we present a straightforward method for producing high-purity (up to 97%) polymeric sporopollenin biocapsules (S-BioCaps) from bee pollen, exploring new plant sources for S-BioCaps, and diversifying the available morphologies to broaden the applications of pollen-based microcapsules. Following a purification process involving defatting, acidolysis, and several washing steps, we removed the inner components of the pollen grains and reduced the protein content to 2%. Confocal laser scanning and scanning electron microscopy images showed that the hollow and 3D S-BioCaps microstructure were preserved, while laser diffraction particle size analysis validated their monodisperse distribution across each pollen type within the size range of 15 to 24 µm. S-BioCaps tended to exhibit hydrophobic behavior when assessed through water dispersion and water marble analysis. Moreover, we sought to figure out the chemical changes occurring in specimens through Fourier-transform infrared analysis, and findings were consistent with simultaneous thermal analysis, where the thermal decomposition of sporopollenin biopolymer reached up to 457 °C. Overall, this work demonstrates a straightforward approach for utilizing pollen grains from *Echium* sp., *Jasione* sp., *Papaver* sp., Amaranthaceae, and *Helianthemum* sp., collected with the assistance of honeybees, to produce stable S-BioCaps with diverse morphologies, thereby broadening their potential applications as drug delivery microcarriers.

Keywords Bee pollen · Renewable source · Polymeric microcapsules · Green carriers

1 Introduction

Over the last few decades, the research interest in the fabrication of integrated chemical structures has increased, with one of the most prominent efforts being the construction of micro-scale hollow structures surrounded by a shell, known as microcapsules [1]. These spheroidal microstructures have been of long-standing interest in various fields, including the encapsulation and delivery of desired active substances in pharmaceutical science [2, 3]. Beyond their role as carriers, microcapsules hold great promise in manifold engineering applications, such as energy storage systems [4],

✉ Miguel Vilas-Boas
mvboas@ipb.pt

1 CIMO, LA SusTEC, Instituto Politécnico de Bragança, Campus de Santa Apolónia, 5300-253 Bragança, Portugal

2 LAQV-REQUIMTE, Departamento de Química e Bioquímica, Faculdade de Ciências, Universidade do Porto, 4169-007 Porto, Portugal

3 PerMed Research Group, Center for Health Technology and Services Research (CINTESIS), Rua Doutor Plácido da Costa, 4200-450 Porto, Portugal

4 Centre for the Research and Technology of Agro-environmental and Biological Sciences, CITAB, Laboratório Apícola – LabApis, Departamento de Zootecnia, Universidade de Trás-os-Montes e Alto Douro (UTAD), 5000-801 Vila Real, Portugal

5 CINTESIS@RISE, Faculty of Medicine, University of Porto, Alameda Professor Hernâni Monteiro, 4200-319 Porto, Portugal

6 Department of Community Medicine, Health Information and Decision (MEDCIDS), Faculty of Medicine, University of Porto, Alameda Professor Hernâni Monteiro, 4200-319 Porto, Portugal

Published online: 27 January 2025

catalytic reactions [5], separation technology [6], food [7], and emulsion technology [8].

Significant advances have been achieved in the preparation and application of microcapsules through different techniques, including in situ and interfacial polymerization, layer-by-layer assembly, self-assembly, spray drying, sol-gel encapsulation, cryogenic solvents, and others [1]. Nevertheless, the fabrication of sophisticated three-dimensional microcapsules with such a large internal cavity and in particular uniform size, porosity, and architecture is costly and complex, posing a significant challenge [2, 9]. Concurrently, the use of greener strategies by using less material, chemicals, and energy along the microcapsule production technology is to be considered [10, 11]. The approaches mentioned above are based on producing complex chemical structures from scratch, however, nature's ability to create complex biological systems provides diverse micron-scale bioparticles with a variety of sizes and morphologies under different dynamic and environmental conditions. Inspired by this, scientists are striving to use the biomass supplied by nature, as a useful and sustainable resource for the design and production of nano- or micro-scale functional materials [11].

Pollen grains represent a promising alternative for designing such systems. Pollen is a unit for transporting and discharging male gametes (or sperm cells) into female gametophytes for sexual reproduction in higher plants, generally consists of a pollen wall and protoplast [12]. The natural role of the pollen wall is to protect the plant's genetic material against ultraviolet irradiation, desiccation, microbial attack, and unfavourable environmental conditions, including mechanical stress and chemical degradation thanks to its double-layered wall called exine (outer layer) and intine (inner layer) [6, 9]. Exine is made up of a crosslinked biopolymer called sporopollenin, while intine consists mostly of cellulose and pectin [13]. Sporopollenin microcapsules purified from pollen grains are one of the unique chemically and mechanically stable naturally occurring biomaterials holding uniform size and porosity and large internal spaces, making them a promising material [3, 14]. These features are major reasons why sporopollenin-based biocapsules are utilized for transporting pharmaceutical drugs [15–17], proteins [18, 19], and living cells [20], along with other applications, for example, biotemplates [21], environmental remediation [22] and 3D printing materials [23].

Plants are frequently regarded as a major renewable resource for the production of sporopollenin biocapsules (S-BioCaps) with desired morphological properties. Nevertheless, few studies highlight the potential of bee pollen, but they exclude the collection, processing, and purification steps required to obtain the desired pollen species [13, 24]. Tan et al. [14] reported treating commercially available bee pollen pellets from the *Camellia sinensis* plant origin, transforming them from hydrophobic into super hydrophilic microcapsules. Another study revealed that using a single type of bee pollen grains (*Camellia*, rape seedflower, or sunflower) purchased at a local market greatly facilitated the production of monodisperse w/o Pickering emulsion droplets [8]. However, to date, no study has fully described the process of harvesting bee pollen pellets and transforming them into functional biomaterials. Thus, we present a comprehensive method that encompasses the entire process and further explore novel S-BioCaps with various sizes and morphologies derived from bee pollen pellets, aiming to expand the applications of pollen-based natural microcapsules in fields ranging from pharmaceutical research to food science. Five selected pollen types—*Echium* sp. (Ech), *Jasione* sp. (Jasi), *Papaver* sp. (Pap), Amaranthaceae (Ama), and *Helianthemum* sp. (Hel), previously unexplored, were chosen for their representation of a wide diversity of floral resources among species frequently visited by bees. Besides, these pollen types exhibit diverse morphological properties and are technically accessible for separation by color.

Bee pollen emerges to be an animal end product, albeit of plant origin. Foraging bees process the pollen grains collected from flowers into moist bee pollen pellets by blending them with some nectar and their secretions, and stick the pellets to the pollen basket on the hind legs of the bees allowing the transport to the hive [12, 25, 26]. Each bee pollen pellet usually consists of the same plant species, with an average diameter of 3–5 mm and a fresh weight of about 15 mg [26]. This feature of pollen pellets is the key to the fabrication of large amounts of identical microcapsules. All that needs to be done is to place a pollen trap at the entrance of the hive, and the bees do the rest flawlessly [12]. Furthermore, using bee pollen for S-BioCaps production may provide some benefits, including the possibility of simultaneous production of different pollen species from a single apiary with reduced energy and labor requirements in a short time. Bee pollen is also a low-cost raw material that could be processed on an industrial scale, with a significant economic impact on global markets [25]. Bees not only collect pollen but also provide essential ecosystem services as pollinators of food and wild crops [25]. Additionally, bee pollen has been consumed since ancient times as a functional food with nutritional value and numerous health benefits [12, 27].

Herein, motivated by the advantages of bee pollen and the spectacular role of pollen grains in nature, we have developed an approach to describe how a product from the beehive is converted into a useful biomaterial. This way elucidates the process from the initial trapping of pollen pellets, their separation by their colour and morphology, following the fabrication and characterization of robust hollow

S-BioCaps. This approach could drastically reduce the collection/processing requirements for producing microcapsules by managing a hive (or apiary) while ensuring high purity of different sizes, uniformity, and surface ornamentation from a single point in a short timeframe.

2 Experimental section

2.1 Bee pollen collection and preparation

Bee pollen specimens were collected from *Apis mellifera iberiensis* colonies in Bragança (northeast Portugal) and Nisa (east-central Portugal) between April and August 2022, coinciding with the blooming period of plant species that produce the desired types of pollen. Pollen traps were placed at the entrance of each hive to ensure the collection of pollen pellets as the bees returned from foraging trips. The traps were designed to minimize stress to the bees while effectively capturing pollen loads. Bee pollen was harvested every two days to reduce the risk of deterioration or contamination due to environmental factors (e.g., humidity, and temperature fluctuations). Upon collection, the harvested bee pollen pellets were manually cleaned to remove extraneous materials, including wood residues, dead bee parts, and other contaminants. A two-step cleaning process was employed: first, gross impurities were removed by hand sorting, followed by sieving using a sieve to ensure finer debris was eliminated. The cleaned pollen specimens were then subjected to microscopic analysis using a Nikon Microphot-FXA microscope (Nikon Co., Tokyo, Japan) to identify the pollen species based on their main colors. Each type of pollen was classified according to its specific color, and shape. This identification process was facilitated by referencing a palynological database for the region, which enabled accurate species-level identification. Following species identification, pollen pellets of interest were sorted based on both shape and color under daylight conditions to ensure accurate differentiation between pollen pellets. The color sorting process was conducted and each specimen was carefully examined to minimize cross-contamination between pollen species. The sorted pollen pellets were stored at −22 °C in sterile containers to preserve their integrity for further chemical processing. Specimens were maintained at this temperature to prevent enzymatic degradation or moisture-related spoilage, ensuring their stability throughout the experimental procedures.

2.2 Palynological analysis

For quality assurance, the accuracy of the color-based sorting and the botanical origins of the bee pollen specimens were confirmed by additional palynological analysis. Briefly, 2 g of bee pollen was mixed with 20 mL of water in a Falcon tube, then vigorously mixed to obtain a homogeneous disaggregate sample and allow a representative sub-sample. 0.4 mL of the resulting mixture was taken and centrifuged at 3500 × *g* for 15 min. The resulting pellet was subjected to acetolysis as previously reported [28]. Pollen identification and counting were accomplished by using an optical microscope (Nikon Microphot-FXA, Nikon Co., Tokyo, Japan). More than 900 pollen grains were counted per preparation according to Van der Ohe et al. [29].

2.3 Defatting of bee pollen and extraction of S-BioCaps

Bee pollen specimens were subjected to a series of treatments with acetone, water, and diethyl ether, according to previously reported methods [14, 30], to remove pollenkitt, a sticky material consisting mainly of lipids, flavonoids, carotenoids, and polysaccharides, which cover the outer layer of the pollen grains. Approximately 50 g of bee pollen was transferred to a round bottom flask with a magnetic stirring bar, connected to a reflux condenser with a water circulation system and water bath, and refluxed in 400 mL of acetone (50 °C, 220 × *g*) for 3 h. After the supernatant was decanted, the sample was washed with 400 mL of warm water (50 °C, 220 × *g*) for 1 h, under stirring, until the bee pollen aggregates were into individual particles. This process was repeated twice. The resulting sample was refluxed in 400 mL of acetone (50 °C, 220 × *g*) for 3 h. After decantation, the sample was left to air-dry for 12 h in a fume hood. The dry sample was stirred in 400 mL of diethyl ether (room temperature (RT), 300 × *g*) for 2 h, and the procedure was repeated. The sample was then mixed with 400 mL of fresh diethyl ether (RT, 300 × *g*) on a magnetic stirrer for 12 h. After the supernatant was removed, the sample was left to dry in a fume hood for 12 h. For each supernatant removal step described above, the pollen particles were collected using a vacuum pump filter system (Model DA7C, Charles Austen Pumps Ltd., Byfleet, UK), passing the pollen grains through a glass filter funnel with the sintered disc with ⌀5–15 µm porosity grade (Büchner funnel-BFU3-20D-001, Glassco Co., Ambala, India).

For extraction of S-BioCaps, previously defatted pollen grains were subjected to acidolysis in 400 mL of 85% (w/w) phosphoric acid (70 °C, 250 × *g*) for 8 h as elsewhere described [13, 14, 30], with slight modifications. After, the S-BioCaps were subjected to an eighteen-step wash process consisting of 400 mL portions: water (50 °C, 5 times), acetone (50 °C, 2 times), 2 M hydrochloric acid (50 °C, 1 time), 2 M sodium hydroxide (50 °C, 1 time), water (50 °C, 5 times), acetone (50 °C, 1 time), ethanol (50 °C, 2 times) and water (50 °C, 1 time). S-BioCaps were collected by vacuum filtration after each washing step. S-BioCaps were transferred to a glass Petri dish (15 cm diameter) and allowed to dry in an oven (Memmert UNE400, Schwabach, Germany) at 45 °C for 3 days. The dried S-BioCaps were then stored in a desiccator, containing silica gel.

2.4 Total protein content analysis

The total nitrogen contents of both bee pollen and extracted S-BioCaps were determined according to the macro-Kjeldahl technique using a Kjeldahl steam distillation unit (Pro-Nitro A, JP Selecta, Barcelona, Spain). The protein contents of the specimens were calculated using the nitrogen concentration and total Kjeldahl nitrogen conversion factor (6.25), following the recommendations of the Association of Official Analytical Chemists, as follows [31]:

$$Protein = Nitrogen\ (\%) \times 6.25$$

2.5 Environmental scanning electron microscope

The surface morphology and structural integrity of untreated, defatted, and S-BioCaps were characterized with scanning electron microscopy (SEM), FEI Quanta 400 FEG ESEM/EDAX Genesis X4M (FEI Inc., OR, USA) instrument at 15.00 kV acceleration voltage under various magnifications. For imaging, specimens were spread on conductive carbon tapes and coated with Au/Pd using sputter coater equipment (SPI Module Sputter Coater, PA, US) (15 mA, 100 s).

2.6 Laser diffraction particle size analysis

The particle size and particle size distribution of the S-BioCaps were measured using a Mastersizer 3000 (Malvern Panalytical Inc., Malvern, UK) based on the laser diffraction technique [32]. An average of five measurements was taken at 22 °C, with distilled water as the dispersion medium. The determined parameters were D_{10}, D_{50}, and D_{90}, representing the particle sizes corresponding to 10%, 50%, and 90% of the total particle volume in the specimen, respectively.

The circularity and aspect ratio of the S-BioCaps were calculated from images taken for each specimen using a microscope (Nikon Microphot-FXA, Nikon Co., Tokyo, Japan) and analyzed with ImageJ software (1.53k, MD, USA). Measurements were conducted on 100 randomly selected pollen grains per specimen.

2.7 Confocal fluorescence imaging

Since the sporopollenin wall of pollen is of an autofluorescence nature, it allowed the observation of both treated and untreated pollen using confocal laser scanning microscopy (CLSM). Specimens were spread on a glass slide with a drop of epifluorescence mounting medium (Vectashield®, Vector Laboratories, CA, USA) containing 4’−6-diamidino-2-phenylindole (DAPI), mounted with a coverslip and stored in the dark at 4 °C until observation. LSM 510 META with a Zeiss Axio Imager Z1 (Carl Zeiss, Germany) and the LSM 510 software (version 4.0 SP2) were used to acquire confocal images. The same settings were applied to all images for results normalization. The lasers used were argon (488 nm) set at 13%, helium–neon (543 nm) set at approximately 51%, and diode (405 nm) set at approximately 69%. The pinhole was set to 96 mm (1.02 airy units) for the argon laser, 102 mm (0.98 airy units) for the helium–neon laser, and 112 mm for the diode laser using a 63× objective. Images were captured at a scan speed of 6 or 8 with 1 µm thick Z sections, deconvolutioned using the 3D deconvolution tool of the AutoQuant X3 software (Media Cybernetics, MD, USA), and processed in TIFF images with ImageJ (1.47 v, MD, USA).

2.8 Fourier-transform infrared spectroscopy

Fourier-transform infrared (FTIR) spectra were obtained using a PerkinElmer Spectrum BX FT-IR system (Perkin Elmer Inc., MA, USA) equipped with a diamond attenuated total reflection (ATR) accessory (GladiATR, PIKE Technologies, WI, USA). Reflectance spectra were collected at a spectral resolution of 4 cm^{-1}, by 64 times scanning per measurement over the range from 4000 to 600 cm^{-1}. Background spectra were collected before reading. Data were processed using the PerkinElmer Spectrum v5 software (Perkin Elmer Inc., MA, USA).

2.9 Preparation of water marbles and distribution of S-BioCaps in water

Water marbles were prepared by rolling a small amount of distilled water droplet (typically 10 µL; pH = 7.1; temperature = 22.8 °C) on a bed of dry S-BioCaps placed in a hemispherical watch glass [33, 34]. Immediately after formation, the liquid marble was rolled onto a clean glass slide, and photographs were taken with a digital camera (Canon EOS 600D, Canon Inc., Tokyo, Japan). To visualize the distribution of S-BioCaps in water, approximately 10 mg of the specimen was vortexed with 2 mL of distilled water for 10–15 s. Photographs were taken immediately after vortexing and again after 30 min.

2.10 Simultaneous thermal analysis

The thermal degradation behaviour of bee pollen and S-BioCaps was evaluated using thermogravimetric analysis (TGA), derivative TG (DTG), and differential thermal analysis (DTA) with an STA7200RV Simultaneous Thermal Analyzer (STA) System (Hitachi High-Tech Inc., Tokyo, Japan). Specimens were heated from 20 to 700 °C at a scan rate of 10 °C/min. Data were analyzed using the TA7000 software (Hitachi High-Tech Inc., Tokyo, Japan).

2.11 Data analysis

The statistical software GraphPad Prism version 9.3 (San Diego, CA, USA) was used for data analysis. Data were compared using a two-tailed *t*-test, and $p < 0.05$ was considered significant.

3 Results and discussion

3.1 Isolation of S-BioCaps from bee pollen

One of the main goals of the work was to develop a pathway that involves harvesting bee pollen pellets from the apiary to fabricate different types of protein-free hollow microcapsules, Fig. 1. To achieve this, it was necessary to evaluate some critical factors that allow the collection of the desired pollen species: (i) the flowering periods of the plants in the area where the apiaries were established, and (ii) which plant species the bees visit and collect pollen in abundance.

Palynological analysis of the bee pollen pellets demonstrated that after sorting the pollen pellets based on morphological features and color, Fig. 2a and Table S1, each group represented pollen from a single botanical origin. These findings suggest that honeybees typically collect pollen grains from the same plant species to form individual bee pollen pellets [12, 35]. By contrast, if foraging bees have difficulty finding enough pollen from a plant, they may visit multiple plants to form a single pellet [36]. This behaviour would eventually impede the production of high-purity microcapsules from bee pollen pellets composed of a single plant origin. However, such cases are rare and usually occur in the later stages of the flowering season. Honeybee colonies do not sustain large amounts of stored pollen, instead, bees actively and delicately regulate the amount of pollen in congruence with the colony needs and particularly the amount of uncapped brood (eggs and larvae) [25, 37]. Even though bee colonies do not usually experience pollen shortages, the colonies may sometimes need more pollen. It is also worth pointing out, that long-term pollen trapping and colony manipulation to obtain the desired raw material should be managed by beekeepers to eliminate the negative consequences on colony productivity, population size, and survival [25, 26, 38].

The finding also showed that although the pollen pellets have a uniform colour, up to 97% of pure product was achieved for all the types of pollen, Fig. 2a and b. This observation suggests that any contamination is not due to

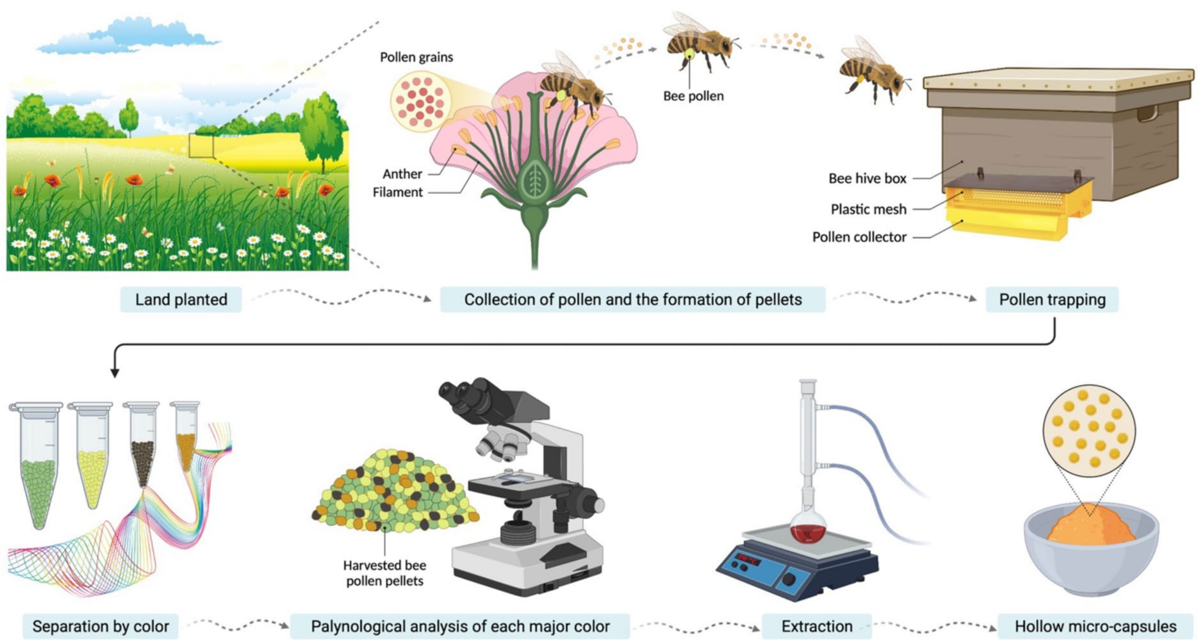

Fig. 1 Outline flow diagram showing the pathway from the collection of bee pollen from the hive, which is a natural resource by exploiting bees, to the production of S-BioCaps

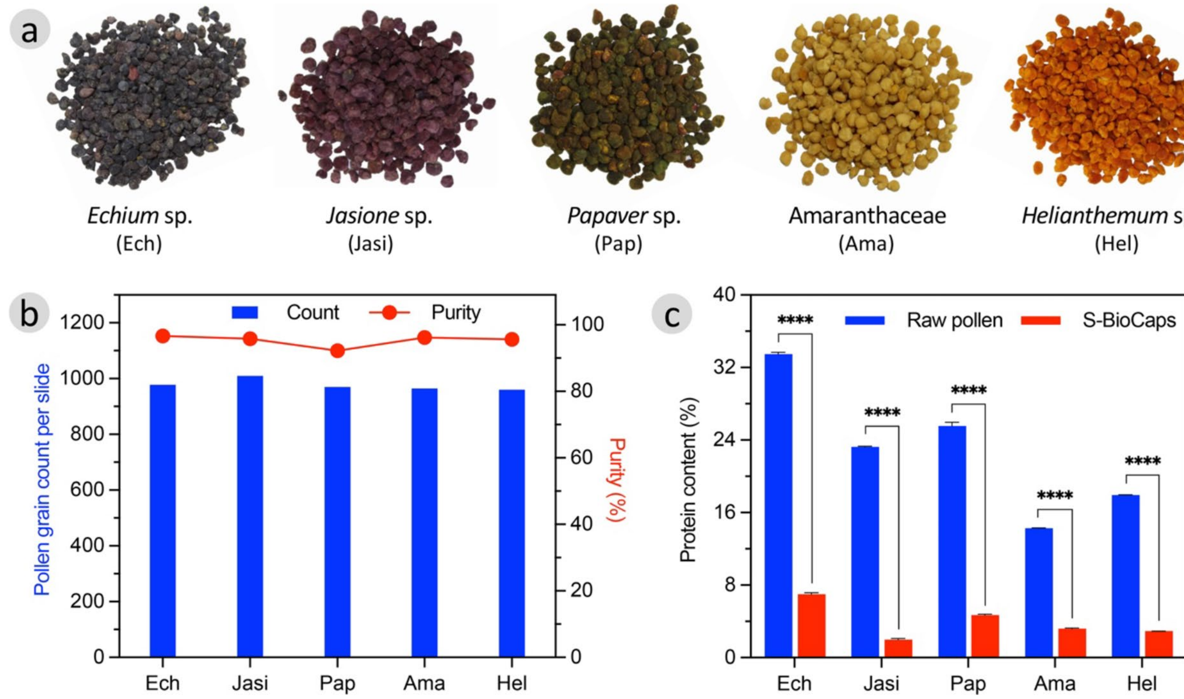

Fig. 2 (**a**) Separation of pollen pellets from polyfloral bee pollen by their color/morphology and results of the palynological analysis on their botanical origin. (**b**) Purity ratios of the bee pollen were obtained from the same analysis. (**c**) The protein content of bee pollen and S-BioCaps. Crude pollen pellets showed a dramatic decrease in protein content after chemical treatment. Data are the mean of three independent measurements *($n=3$)* with ±SD. The *t*-test was performed for comparison. **** = $p<0.0001$

the bees' pollen collection behaviour but rather to physical mixing in the pollen trap collector, where moist pollen pellets may come into contact with each other, or from the presence of different types of pollen with very similar colors, as seen in the Pap specimen (Fig. 2a). Nevertheless, selecting specific production periods and carefully sorting the bee pollen pellets by color enabled the production of highly pure products, with purities ranging from 92% (Pap) to 97% (Ech) (Fig. 2b). Additionally, contamination could be minimized by gently handling the pollen pellets during collection, drying, and sifting to detach any adhering pollen grains from other pellets. However, it is worth noting that drying may cause the release of cytoplasmic materials from the pollen grains.

We employed a well-defined chemical purification method to obtain intact and hollow S-BioCaps from the colour-sorted bee pollen pellets (see Section 2). This method involved defatting, followed by acidolysis using 85% (v/v) phosphoric acid and a series of washing steps. The 8-hour acidolysis time was sufficient for all types of pollen to remove the protein, lipid, and cytoplasmic substances while opening the apertures on the pollen wall. After the defatting, acidolysis, and washing procedure, the yield of S-BioCaps from bee pollen pellets was 14.3%, 6.1%, 9.6%, 11.6%, and 10.7% for Ech, Jasi, Pap, Ama, and Hel species, respectively.

The validation of proteinaceous material removal from the pollen grains was based on nitrogen quantification in the purified S-BioCaps [39–41] using a conversion factor of 6.25 to estimate total protein content [39, 40]. The analysis showed a significant ($p<0.0001$, *t*-test) reduction in the protein content of the S-BioCaps after the chemical treatment of the bee pollen, Fig. 2c. The method successfully removed proteinaceous material from the five types of pollen, with removal rates ranging from 79% (Ech) to 91% (Jasi). The amount of measured nitrogen was assumed to originate entirely from proteins, but the influence of the nitrogen content of the structural component of the pollen wall should be also considered when evaluating removal efficiency [41, 42]. The measured values are similar to those previously reported in the literature [14, 18, 40, 43, 44]. Given that proteins are commonly associated with pollen-based allergic reactions [41], this significant reduction in protein content suggests the potential for minimizing allergens. Moreover, since bee pollen is consumed as a dietary supplement [12], these pollen-derived S-BioCaps could serve as promising candidates for oral drug delivery systems [2].

3.2 Morphological characterization

Each type of pollen has its own 3D structure and specific surface architecture, which may be altered during the chemical treatment [30, 40, 43]. Therefore, SEM was employed to investigate the surface morphology of the raw, defatted, and purified S-BioCaps. The SEM images in Fig. 3 show that the structural integrity of all S-BioCaps remained intact after treatment and with no visible damage, and the nanoscale architecture of the sporopollenin wall was preserved across all specimens. The key reason behind the successful preservation of the S-BioCaps morphology lies in the inherent robustness of sporopollenin. The chemical stability of this biopolymer, composed of aromatic rings and long-chain fatty acids, enables it to withstand harsh processing conditions, such as acidolysis and defatting, without significant alteration to its structural features [45]. Notably, certain regions in raw pollen, especially at the apertures, the exine layer is either thin or absent and supplanted by the intine layer [46]. These sites are naturally the weakest

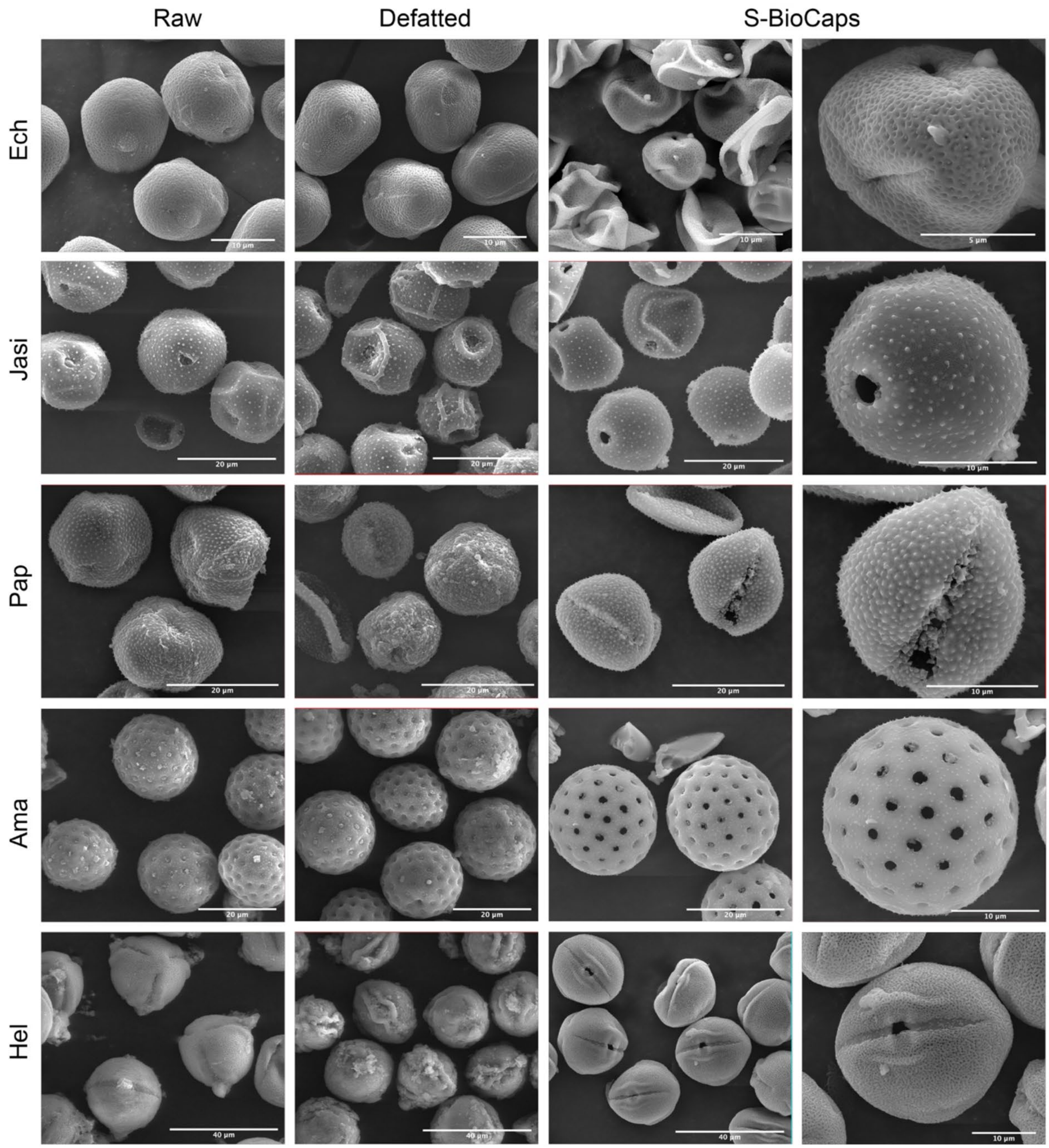

Fig. 3 Scanning electron micrographs of different types of pollen grains before and after chemical treatment. The first column shows images of untreated pollen grains. The second column shows the shrunken pollen grains and still closed openings after defatting. The third and fourth columns at different magnifications show the opened apertures located on the pollen wall and also intact and clean microcapsules after acidolysis

because they evolve to allow the pollen tube to emerge from the pollen during fertilization [42, 47]. The opening of these apertures after the treatment is a critical feature for potential applications, such as the encapsulation of pharmaceuticals or active substances within the hollow S-BioCaps. The SEM images also revealed that the prolate-heteropolar-shaped Ech S-BioCaps had a perforated surface, while the others presented a spherical shape and perforate/microechinate and striate surface decoration, Table S2.

Laser diffraction particle size analysis and optical microscopy were used to evaluate the micrometric characteristics of the S-BioCaps. Each graph (a-e) in Fig. 4, stands for the histogram data and relevant fitted Gaussian curves of S-BioCaps diameter size distribution as a function of volume (%). The laser diffraction data further validates the monodispersity achieved by color-based pollen separation, which simplifies the production process and results in size-uniform microcapsules suitable for scalable applications. The mean spherical diameters of the purified S-BioCaps were 15.1 ± 0.1 μm (Ech), 17.7 ± 0.0 μm (Jasi), 18.1 ± 0.0 μm (Pap), 23.5 ± 0.1 μm (Ama), and 24.1 ± 0.1 μm (Hel). The detailed values of the particle size distribution in volume (D_{10}, D_{50}, and D_{90}) for each S-BioCaps are summarized in Table S3, with minimum volumes for Ech and Jasi and maximum values for Ama and Hel, up to 30% more.

Figure 4f and g show the circularity and aspect ratio of S-BioCaps, respectively. These parameters were measured after hydrating the S-BioCaps in water to complement the laser diffraction data. Circularity or roundness measures how closely the shape of an object resembles a perfect circle, and the aspect ratio is described as the width: height of an object [10]. The results showed a general decrease in the aspect ratio with an increase in the circularity. The highest circularity value (ideal circle = 1) was observed in Ama S-BioCaps with 0.93 ± 0.01, followed by Jasi (0.91 ± 0.02) and Hel (0.85 ± 0.06). On the other side, Ech has the lowest aspect ratio and a width circularity dispersion, likely due to its original prolate shape. Selecting S-BioCaps based on size, circularity, and aspect ratio, depending on the intended application, can offer specific advantages. For instance, S-BioCaps with a high aspect ratio might enhance interaction with epithelial cells in the intestinal lumen, extending their residence time and potentially improving drug release due to increased adhesivity and other beneficial properties.

The changes in the macromolecule presence between the natural pollen grains and the S-BioCaps were investigated using a confocal microscope, particularly to identify and qualitatively visualize their localization. Pollen grains are naturally fluorescent over a wide range of emission wavelengths from blue to red [10, 48, 49]. This autofluorescence allowed visualization of both the pollen wall and inner cavity by employing a suitable combination of excitation-emission filters. CLSM images of natural pollen grains generally showed stronger autofluorescence in the blue and green channels throughout the pollen cavity, with relatively weaker signals in the red channel. The fluorescence was more pronounced in the overlay images, Figs. 5 and S1.

This autofluorescence could be attributed to the presence of cellular components in the inner cavity of the pollen grains [40, 49, 50]. Moreover, some natural pollen grains fluoresced more subtly than others, evidencing the possibility that part of the liquid cytoplasmic components may leak out during the collection and drying of the bee pollen pellets. Conversely, in the S-BioCaps images, no autofluorescence was detected from their inner cavity, indicating effective removal of biomacromolecules. The pollen wall,

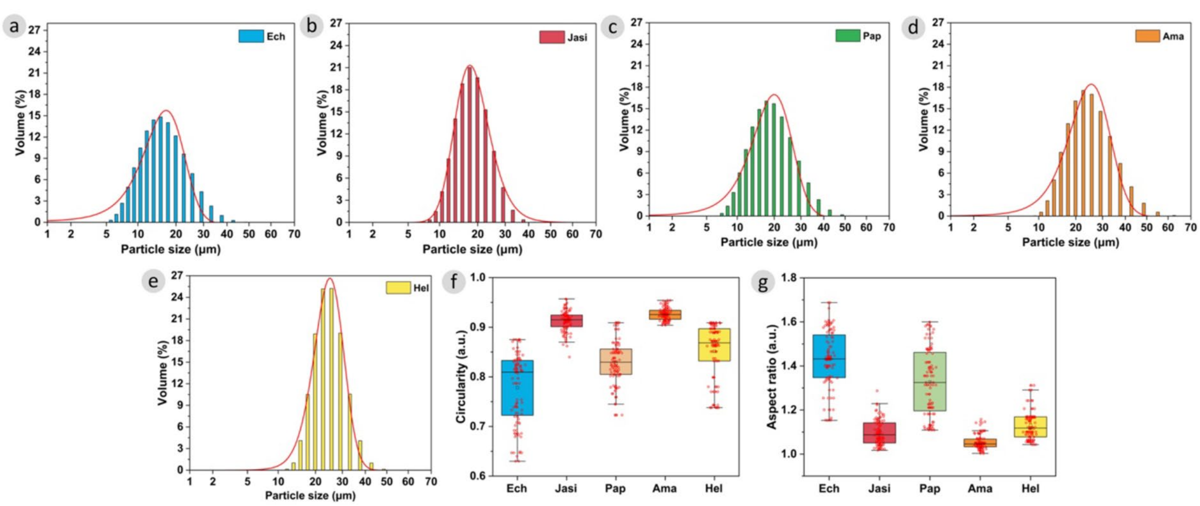

Fig. 4 Micrometric properties of S-BioCaps analyzed with laser diffraction particle sizer. **(a–e)** Graphs from curve fitting to histograms for the equivalent spherical diameter of the size distribution of five different types of pollen after five measurements ($n = 5$). **(f–g)** the box plots show the circularity and aspect ratio of S-BioCaps, respectively. For box plots, the results represent data from 100 randomly selected pollen grains

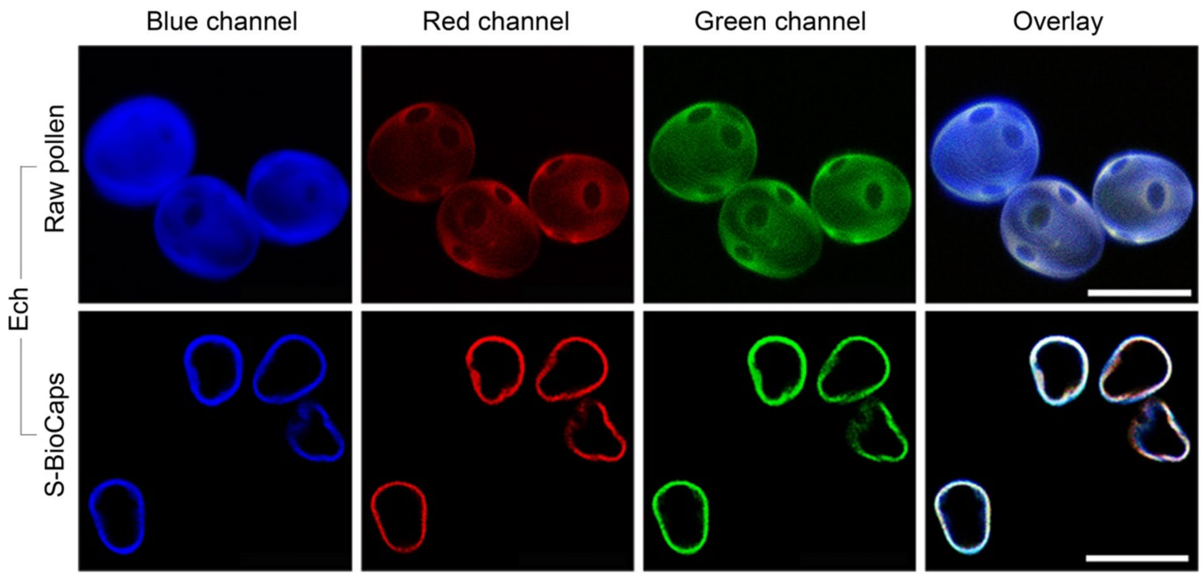

Fig. 5 Confocal micrographs of raw pollen and S-BioCaps from *Echium* sp. (Ech) specimen. Natural and treated Ech show autofluorescence in their inner cavity and the wall at different wavelengths of light. Confocal micrographs of other samples are given in Figure S1, see Supporting information. Scale bar = 20 μm

however, showed intense autofluorescence across all channels, which became more pronounced in the merged images, manifesting as bright yellow or orange fluorescence localized to the pollen wall. This suggests that the cytoplasmic content was effectively removed, leaving behind empty but morphologically stable S-BioCaps. The morphological stability across different species underscores the applicability of S-BioCaps as versatile biomaterials. While the variation in size and shape offers customization options for specific uses, such as drug delivery or environmental remediation, the core sporopollenin structure remains a reliable foundation for functional biomaterials.

3.3 Fourier-transform infrared spectroscopy

FTIR spectroscopy was employed to understand the chemical changes between raw bee pollen and the processed S-BioCaps. Functional group assignments in the spectra were made with reference to previous studies [13, 16, 18, 30, 39, 44, 46, 48, 51, 52]. Figure 6 revealed significant differences between the spectra of the natural pollen grains and the defatting/H_3PO_4-treated S-BioCaps. One of the notable distinctions was observed at the 3300 cm^{-1} band assigned to O–H stretching vibration (hydrogen bonded) in carboxylic acids, alcohol, carbohydrates, or water. After chemical treatment, this broad vibration shifted to 3340 cm^{-1} and decreased in intensity. This reduction suggests the removal of–OH containing compounds during the treatment, including lipids or carbohydrates, and/or the reduction of adsorbed moisture [39, 48]. The peaks observed at 2926 and 2852 cm^{-1} were related to the asymmetric and symmetric C–H stretching vibrations of methylene groups ($-CH_2-$), associated with carbohydrates. Intensities of these aliphatic vibrations did not appear to decrease significantly after 8 h of H_3PO_4 treatment.

Further changes were observed in the 1700–800 cm^{-1} region of the spectra. The peak at 1740 cm^{-1} in the bee pollen was assigned to the carbonyl (C═O) stretching of the aliphatic ester groups of fatty acids and/or lipids. Reported work on *Lycopodium clavatum* stated that this vibration was present at the end of the 6 h acidolysis following the 8 h defatting treatment with n-hexane [48]. Here, however, this vibration disappeared after the defatting step of acetone and diethyl ether treatment (Fig. S2) and did not reappear after the acidolysis, indicating that all S-BioCaps specimens were lipid-free, Fig. 6.

The vibrations at 1638, 1548, and 1238 cm^{-1}, important regions associated with the presence of proteins in natural pollen, were assigned to the C═O stretching in the amide I, N–H bending and C–N stretching in amide II, and N–H bending, C–N, and C–C stretching in amide III, respectively [18, 51, 52]. For the latter, we cannot exclude the possible contribution of PO_2^- from nucleotides (DNA, RNA) [18, 51, 52]. These vibrations disappeared after the H_3PO_4 treatment. The disappearance of these peaks in the spectra of S-BioCaps clearly shows that the acidolysis process removed protein content significantly, as confirmed by the Kjeldahl nitrogen analysis. Peaks at 1660 and 1511 cm^{-1} in S-BioCaps were assigned to the asymmetric stretching of the non-conjugated C═C owing to aromatic and phenolic compounds in sporopollenin [51], while vibrations at 1412 and 1570 cm^{-1} in natural bee pollen and S-BioCaps were

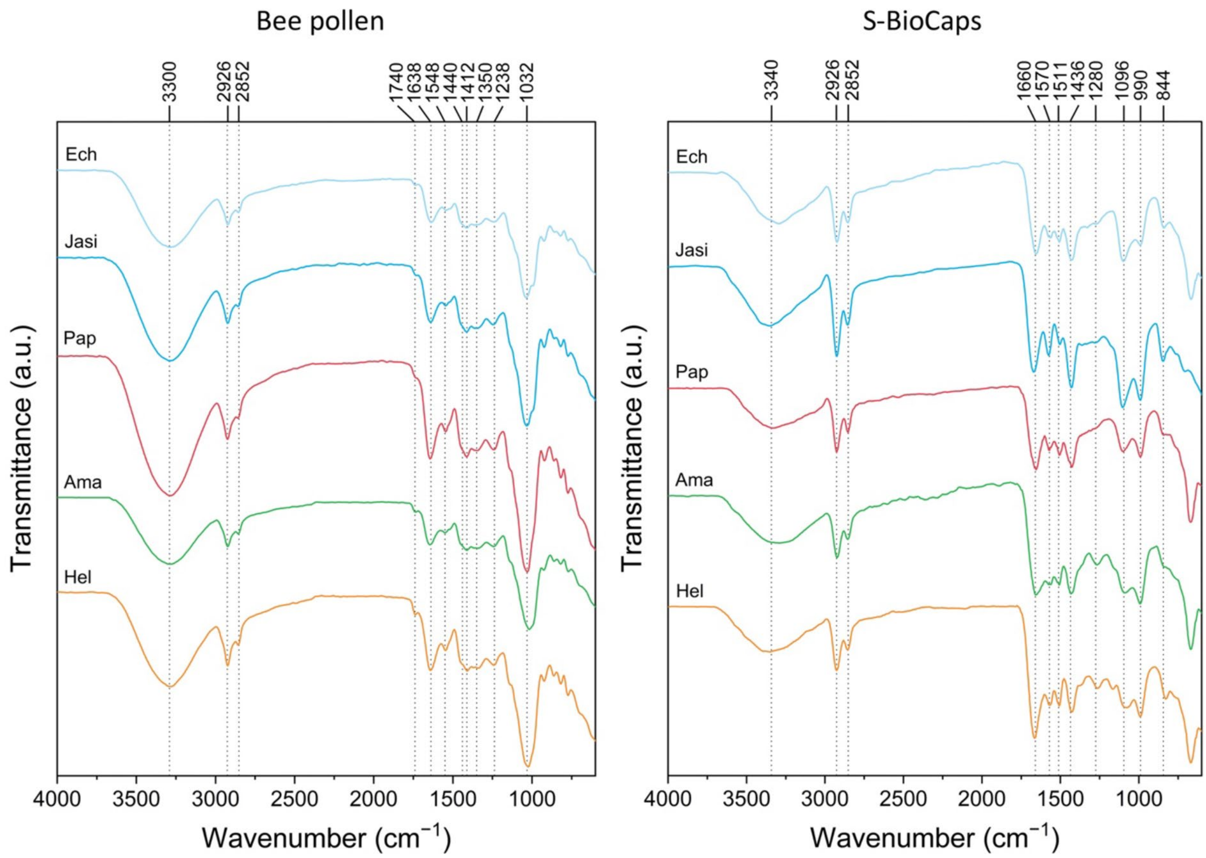

Fig. 6 FTIR spectra of bee pollen and S-BioCaps after chemical treatment and a series of washing steps

attributed to symmetric and asymmetric stretching in carboxylate anions (COO^-), respectively [39, 51]. These carboxylic groups play a crucial role in the functionalization of S-BioCaps, as they can serve as reactive sites for future surface modifications.

The vibration at 1440 cm^{-1} attributed to the C–H stretching in the aromatic ring of the sporopollenin was observed in natural pollen grains. The vibrations at 1511 cm^{-1} and 1440 cm^{-1}, attributed to C═C and C–H stretching in aromatic rings of sporopollenin, confirm the preservation of the biopolymer structure. These peaks reflect the chemical resilience of sporopollenin, which is known for its durability and stability under harsh chemical conditions, including the acidolysis employed in this study. This vibration shifted to 1436 cm^{-1} and became sharper in all S-BioCaps after the chemical treatment. The vibration at 1350 cm^{-1}, assigned to the C–CH_3 bending in carbohydrates, was present in natural and defatting pollen but disappeared after the acidolysis step, Figs. 6 and S2. Besides, acidolysis treatment resulted in the disappearance of the C–O–C stretching vibration observed at 1032 cm^{-1} observed clearly in the bee pollen. It was associated with cellulose abundance, which evidenced the natural pollen cellulose removal/reduction by the H_3PO_4 treatment. The vibration at 1280 cm^{-1} was attributed to the C–O stretching of the alkyl esters, and the intensity of this band was more distinguishable in Ama and Hel S-BioCaps compared to others. Uddin et al. [39] reported that the peak completely disappeared after KOH and H_3PO_4 treatment, but in our study, this vibration was evident for the two aforementioned S-BioCaps types, probably due to pectin-related residues. This could be due to variations in the botanical origin of pollen and the degree of purification achieved. Vibrations at 1096 and 990 cm^{-1} were assigned to the pyranose ring of sugars (skeletal vibrations of C−OH and C−O−C). Finally, the vibration at 844 cm^{-1} in S-BioCaps was attributed to the aromatic ring stretching vibration in sporopollenin [30, 46, 51].

Li et al. [53] reported that the sporopollenin polymer primarily comprises aliphatic-polyketide-derived polyvinyl alcohol units. These units are crosslinked with 7-*O*-*p*-coumaroylated C16 aliphatic chains through a unique dioxane moiety, which is an acetal functional group. In addition to these primary components, sporopollenin contains minor components, such as naringenin, a flavonoid-derived compound. In the same study, solid-state nuclear magnetic resonance spectroscopy identified various carbon environments, including acetal carbons (~ 103 ppm), carboxyl carbons (~ 173 ppm), aliphatic carbons (30–44 ppm), and aromatic carbons (160–110 ppm), further confirming the presence of acetal and ester crosslinks. In another study with FTIR analysis [45], hydroxyl (–OH) groups from alcohols and carboxylic acids were detected, participating in hydrogen bonding and contributing to sporopollenin chemical properties. The polymer also exhibited carbon-carbon double bonds (C=C) from aromatic and alkenyl moieties, primarily originating from phenylpropanoid units like *trans*–4-hydroxycinnamyl. Furthermore, ester linkages (–COO–) were observed, indicating the presence of lipid esters and supporting the hypothesis of a polyhydroxylated structure. The findings support a structural model in which the polymer consists of aliphatic chains crosslinked with phenylpropanoid derivatives, primarily through ester and acetal bonds. This is consistent with the functional groups identified above in our discussion.

Collectively, the FTIR data suggest that the sporopollenin structure, regardless of the botanical source, retains a similar core chemical composition. Characteristic peaks, C═C vibration in the aromatic ring of sporopollenin, asymmetric stretching in carboxylate anions (COO^-), and C–H stretching in the aromatic ring of the sporopollenin, are consistent across specimens. Nonetheless, the intensity and presence of certain peaks vary depending on the extent of removal of other pollen components (e.g., cellulose, pectin, proteins), but may also be influenced by the botanical origin of each S-BioCaps. These results highlight the chemical resilience of sporopollenin, ensuring its durability as a biomaterial in various applications.

3.4 Wettability behaviour of S-BioCaps

Natural pollen grains are primarily hydrophobic, a property generally retained even after chemical purification processes such as acidolysis [14], though some variation can occur depending on the specific treatment applied [39]. The wettability of S-BioCaps is a critical property that influences their behaviour in aqueous environments, particularly in applications like pharmaceutical formulation, drug release, and mucoadhesion [39, 54]. To assess the hydrophilic/hydrophobic behaviour of S-BioCaps after sequential chemical treatments, two qualitative analyses were performed: the formation of water marbles in air coated with S-BioCaps and the dispersion of S-BioCaps in water, as shown in Fig. 7.

Hydrophobic S-BioCaps shaped water marble when particles self-organize at the air-liquid surface of a hydrophilic drop [34], as evidenced by Jasi, Pap, and Ama. For Ech and Hel S-BioCaps, although formed water marbles in a hemispherical watch glass at first, they collapsed as soon as they were transferred to the glass surface (a few attempts were unsuccessful). S-BioCaps were partially dispersed after mixing in water, as shown in Fig. 7 on the right side, but after being kept in a static environment for about 30 min, some of the S-BioCaps sedimented, while others floated on the surface. The two types of S-BioCaps that appeared to be less hydrophobic, i.e., those that did not form water marbles, still did not show a distinctive dispersion in water compared to the others. Similar behaviours were reported in other works and are probably because of the density difference of the particles absorbing water through nanochannels and apertures or related to the wettability of the S-BioCaps [33]. The partial dispersion observed in all S-BioCaps could be explained by the sporopollenin inherent hydrophobicity, which resists complete wetting in aqueous environments, as well as the ability of the surface structure to trap air or water within the perforations.

Beyond morphology, the surface chemistry of S-BioCaps is key to their hydrophobic or hydrophilic behavior [14]. Functional groups on sporopollenin determine particle wettability, and FTIR analysis before and after chemical treatment reveals valuable insights into their water affinity. The functional group densities corresponding to the O–H stretching vibration at 3300 cm^{-1} and the COO^- stretching at 1570 cm^{-1}, which are associated with the hydrophilic properties of the sporopollenin biopolymer, significantly decreased after H_3PO_4 treatment. This reduction might have contributed to the hydrophobic characteristics observed. Furthermore, compared to raw pollen, the sharp peaks at 2926 cm^{-1} and 2852 cm^{-1}, attributed to asymmetric and symmetric C–H stretching vibrations, along with the peaks assigned to C═C stretching (possibly originating from aromatic and phenolic compounds), could be another factor limiting the wettability of the S-BioCaps. The presence and density of surface hydrophilic groups (hydroxyl and carboxyl) and hydrophobic groups (aliphatic and aromatic) vary depending on the chemical treatment. Acid treatments, in particular, have been reported to result in particles with low water affinity, as observed in *Lycopodium clavatum* and pine pollen [39, 55]. Similar to previous studies, the S-BioCaps in this work predominantly exhibited hydrophobic characteristics. However, treatments with NaOH or ultraviolet–ozone could enhance the formation of surface functional groups such as carboxylate (COO^-) and ketone bonds ($R_2C{=}O$), thereby increasing hydrophilicity or even reversing the hydrophobicity [14, 55].

3.5 Thermal decomposition properties

STA analysis was performed to evaluate the thermal decomposition characteristics of bee pollen and S-BioCaps (Figs. 8, S3, and S4). Thermograms (given in Fig. 8a) showed that the raw bee pollen specimens (Ech, Jasi, Pap, Ama, and Hel) lost approximately 92.8%, 97.6%, 96.7%, 95.5%,

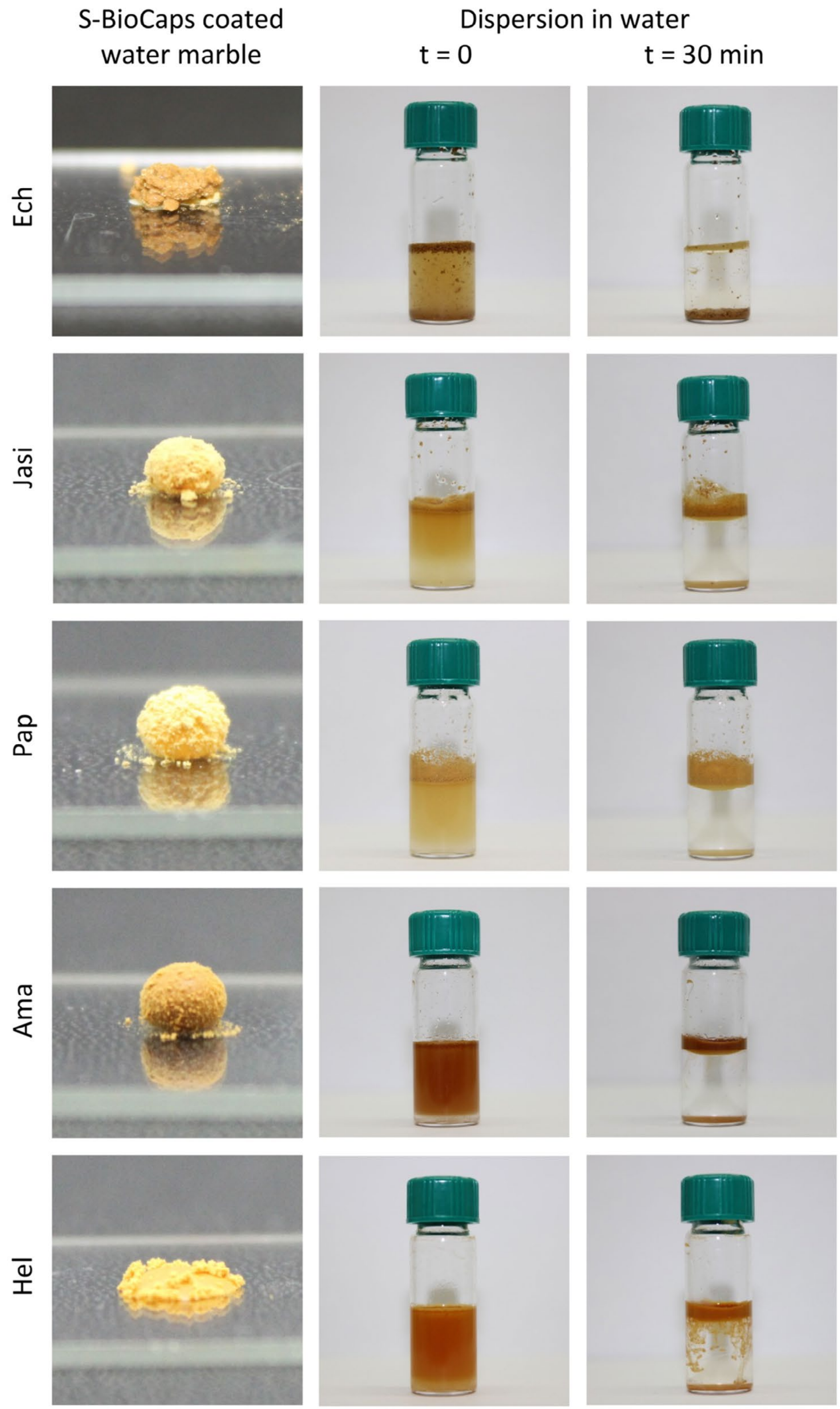

Fig. 7 Wettability of purified S-BioCaps from different types of pollen and their dispersion in water. Photographs in the first column show water marbles stabilized or not by the S-BioCaps in powder form. If the dry powdered S-BioCaps are hydrophobic, the powder spontaneously passes to the water-air interface and thereby does non-wetting and retains the water when transferred to a glass surface. The photographs in the second and third columns show the time-dependent behavior of the S-BioCaps from aqueous dispersion immediately after vortexing and 30 min later, respectively

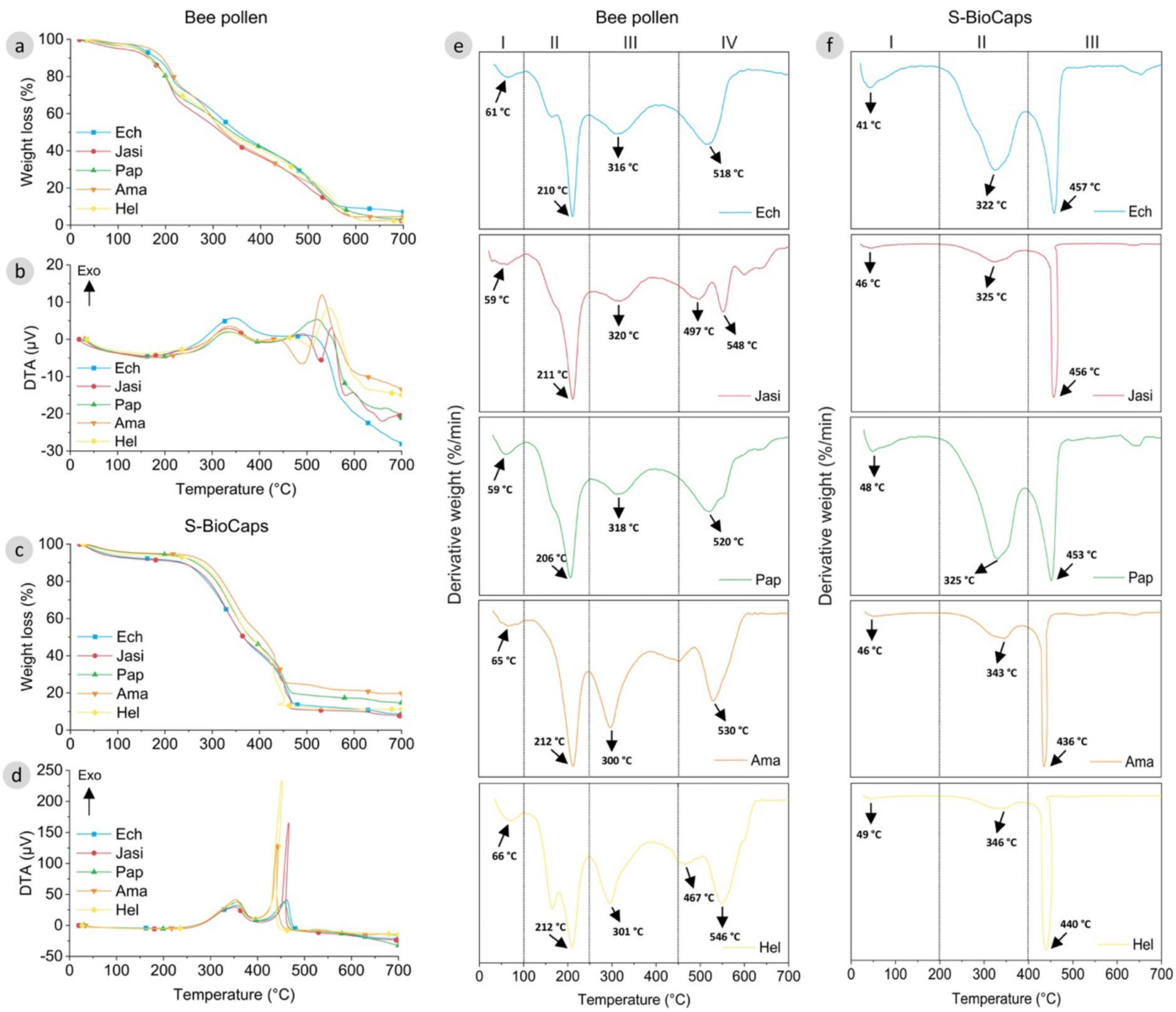

Fig. 8 Thermal decomposition of natural bee pollen and S-BioCaps. (**a**) and (**b**) show TGA and DTA thermograms for raw bee pollen, while (**c**) and (**d**) are for S-BioCaps, respectively. The DTG of natural bee pollen and S-BioCaps were separated into distinct zones and are given in (**e**) and (**f**), respectively

and 97.7% of their initial mass, respectively, upon heating to 700 ºC. These results were slightly higher compared to other studies on pollen collected directly from plants [17, 18, 39, 51]. The higher thermogravimetric reduction in bee pollen could be attributed to the presence of nectar and bee secretions, which are introduced during the formation of bee pollen pellets [12, 26, 36]. In contrast, S-BioCaps exhibited lower weight loss compared to natural pollen: Ech (91.4%), Jasi (92.4%), Pap (85.4%), Ama (80.4%), and Hel (88.8%), Fig. 8c. The presence of cellulose and other wall component residues may alter the thermal degradation profile of sporopollenin [39], as well as differences in weight loss of S-BioCap specimens.

The initial weight loss (zone I) occurred between 34 and 100 °C for raw bee pollen, accounting for a 2–5% decrease in weight, while for S-BioCaps, the weight loss ranged from 5 to 9% in a broader range (34–200 °C). This weight loss can be associated with the removal of weakly adsorbed water with increasing temperature [17]. Weight loss in zone II (100–250 °C) occurred at the decomposition peak around 210 °C. This loss corresponded between 27% and 33% for raw bee pollen, but for S-BioCaps, no decomposition peak was seen in this region, Fig. 8e and f. This event could be attributed to the removal of cellular materials, such as proteins, from bee pollen. Other reports stated the disappearance of the peak in this region after the chemical treatment [48, 51]. Besides, this supports the results of the absence of peaks attributed to the presence of proteins in the FTIR spectrum. Zone III is located between 250 °C and 450 °C. The decomposition peaks around 300–320 °C exhibited loss percentages of 30–41% on the bee pollen specimens, most likely as a consequence of partial degradation of lipids and cellulose [39]. In the same region, S-BioCaps exhibit peaks at slightly higher temperatures, 322 °C to 346 °C, showing weight loss values between 43% and 50%. The absence or minimal presence of proteins, lipids, and wall components would be expected in S-BioCaps. However, noticeable decomposition peaks were observed, especially in the Ech and Pap S-BioCaps, which may indicate the presence of cellulose residues undergoing decomposition [39]. Both specimens showed vibrations attributed to cellulosic components in the FTIR spectra as well, resulting in significantly lower intensity than the corresponding natural bee pollen specimens.

In zone IV (450–700 °C), raw bee pollen specimens exhibited peaks between 518 and 548 °C, with weight losses ranging from 26 to 32%, likely corresponding to the partial decomposition of sporopollenin [16–18, 51]. On the other hand, partial decomposition of the sporopollenin for S-BioCaps occurred at peaks around 436–457 °C, and it accounted for the weight loss of 31–34%. The higher decomposition temperature of sporopollenin in raw bee pollen may be due to the presence of other wall components, such as pectin and cellulose, which enhance structural rigidity. Uddin et al. [39] stated that the presence of cellulose and other components may alter the degradation behaviour of sporopollenin, referring that the decomposition properties of pure materials change with the presence of other components. A similar elucidation was conducted by Alpizar-Reyes et al. [48] for *Lycopodium clavatum* pollen. Altogether, it seems reasonable to assume that the variability of weight loss temperatures between raw and processed specimens, namely bee pollen and S-BioCaps, is related to the removal of specific compounds. A study focusing on the thermal decomposition of sporopollenin and its chemical changes reports that hydroxyl groups (~3450 cm^{-1}) disappear around 360 °C, carbonyl groups (~1710 cm^{-1}) vanish by 500 °C, while aliphatic C–H groups (~2900 cm^{-1} and ~1450 cm^{-1}) diminish but are still detectable at 500 °C [56].

To further elucidate the thermal characteristics of the specimens, we supported them with DTA, Fig. 8b and d. For raw bee pollen, the results showed exothermic peaks in the range of 200–400 °C and exothermic and endothermic peaks in the region between 450 °C and 600 °C. These decomposition peaks were concordant with zones of weight loss of raw bee pollen in the TGA thermograms and their intensity was concordant with weight loss rates on the DTG curves. For S-BioCaps, slightly broad exothermic peaks occurred between 250 and 400 °C whereas sharper exothermic peaks were between 440 and 500 °C, Fig. 8d. These exotherms are associated with two major decomposition peaks, as seen in the TGA and DTG data of S-BioCaps. DTA peaks were attributed to the degradation of various biomass components (lipids proteins, cellulose, hemicellulose, pectin, and sporopollenin) in both natural bee pollen and S-BioCaps [18].

4 Conclusion

In this work, we introduced a novel method to explore pollen grains that serve as raw materials for sporopollenin-based microcapsules using honeybees. Our method simplifies the transformation of pollen into valuable biomaterials, offering advantages such as reduced processing time, lower costs, and scalability compared to traditional methods. This is the first time such a pathway has been proposed. By managing an apiary (or a hive) without affecting the sustainability of the beehive, bee pollen can be easily collected to produce robust S-BioCaps with high purity (up to 97%), after colour separation. The findings evidenced that the apertures located on the surface of the pollen could be opened without damaging their 3D microstructure. Moreover, the cellular materials in the inner cavity could be removed by applying a chemical protocol, resulting in empty S-BioCaps with a variety of morphologies and size homogeneity ranging between 15.1 and 24.1 µm. Infrared spectroscopy pointed out distinct aliphatic and aromatic domains in the chemical structure of sporopollenin from various plant sources. Despite these differences, the overall composition remained similar. Thermal analysis revealed the decomposition temperature of sporopollenin biopolymer was up to 457 °C.

Above all, handling bee pollen as a natural and abundant raw material is an environmentally friendly straightforward way to obtain the desired products from a single area, e.g., an apiary or hive. The key point to consider here is the natural flora where the hive(s) are set up and which plants the bees often prefer to collect pollen. Overall, with an understanding of the potential momentousness of S-BioCaps in medicine and biotechnology, and secondly, for environmental and agricultural applications, the knowledge generated in this research may guide and assist future research.

Supplementary Information The online version contains supplementary material available at https://doi.org/10.1007/s42247-025-01002-1.

Acknowledgements The authors are grateful to the Foundation for Science and Technology (FCT, Portugal) for financial support by national funds FCT/MCTES to CIMO (UIDB/00690/2020 and UIDP/00690/2020), SusTEC (LA/P/0007/2021) and projects: UIDB/50006/2020, UIDB/04033/2020 and UIDP/50006/2020. Thanks to national funding, FCT for CEEC contract (2020.01614.CEECIND/CP1596/CT0007) with Andreia F. Peixoto and the Ph.D. research grant for Volkan Aylanc (2021.07764.BD), and Seymanur Ertosun (2021.08361.BD). Thanks to the NextGenerationEU recovery funds, through the scope of Project BeeLand 10/C05-i03/2021.PPRR-C05-i03-I-000081.

Author contributions Conceptualization: [Cristina Freire and Miguel Vilas-Boas]; Methodology: [Arantzazu Santamaria-Echart, Paulo Russo-Almeida, Seymanur Ertosun and Volkan Aylanc]; Formal analysis and investigation: [Andreia F. Peixoto, Seymanur Ertosun and Volkan Aylanc]; Validation: [Andreia F. Peixoto, Arantzazu Santamaria-

Echart and Paulo Russo-Almeida]; Writing - original draft preparation: [Seymanur Ertosun and Volkan Aylanc]; Writing - review and editing: [Andreia F. Peixoto, Arantzazu Santamaria-Echart, Cristina Freire, Miguel Vilas-Boas, Nuno Vale, and Paulo Russo-Almeida]; Funding acquisition: [Cristina Freire, Miguel Vilas-Boas, and Nuno Vale]; Resources: [Andreia F. Peixoto, Cristina Freire and Miguel Vilas-Boas]; Supervision: [Cristina Freire, Miguel Vilas-Boas and Nuno Vale].

Funding Open access funding provided by FCT|FCCN (b-on).

Data availability All data generated or analysed during this study is included in the article and its ESI.

Declarations

Competing interest The authors declare that they have no known competing financial interests or personal relationships that could have appeared to influence the work reported in this paper.

References

1. M.G. Bah, H.M. Bilal, J. Wang, Soft Matter. (2020). https://doi.org/10.1039/C9SM01634A
2. V. Aylanc, A.F. Peixoto, N. Vale, C. Freire, M. Vilas-Boas, Appl. Mater. Today. (2023). https://doi.org/10.1016/j.apmt.2023.101860
3. C. Zhou, J. Deng, J.H. Tay, S. Basu, J. Yang, J. Li, C. Yang, Z. Zhao, N.J. Cho, Annu. Rev. Chem. Biomol. Eng. (2024). https://doi.org/10.1146/annurev-chembioeng-101121-085959
4. H. Huang, T. Shi, R. He, J. Wang, P.K. Chu, X.-F. Yu, H. Huang, T. Shi, R. He, J. Wang, X. Yu, P.K. Chu, Adv. Sci. (2020). https://doi.org/10.1002/advs.202000602
5. W. Malik, J.P.V. Tafoya, S. Doszczeczko, A.B.J. Sobrido, A.N. Boa, R. Volpe, Sci. Rep. (2024). https://doi.org/10.1038/s41598-024-77780-1
6. Y. Yang, W. Zhang, L. Zhang, M. Guo, C. Xiang, M. Ren, Y. Han, J. Shi, H. Li, X. Xu, Int. J. Biol. Macromol. (2024). https://doi.org/10.1016/j.ijbiomac.2024.133051
7. P.J. Schouten, D. Soto-Aguilar, A. Aldalbahi, T. Ahamad, S. Alzahly, V. Fogliano, Curr. Opin. Food Sci. (2022). https://doi.org/10.1016/j.cofs.2022.100809
8. H. Jiang, H. Yu, X. Guan, W. Jiang, Y. Li, W. Liu, C. Yang, J. Jiang, B.P. Binks, T. Ngai, Adv. Funct. Mater. (2024). https://doi.org/10.1002/adfm.202316510
9. S. Liu, S.Y. Quek, K. Huang, Small. (2024). https://doi.org/10.1002/smll.202403465
10. T. Fan, J.H. Park, Q.A. Pham, E.L. Tan, R.C. Mundargi, M.G. Potroz, H. Jung, N.J. Cho, Sci. Rep. (2018). https://doi.org/10.1038/s41598-018-24336-9
11. C.S. Pomelli, F. D'Andrea, A. Mezzetta, L. Guazzelli, New. J. Chem. (2020). https://doi.org/10.1039/C9NJ05082E
12. V. Aylanc, S.I. Falcão, S. Ertosun, M. Vilas-Boas, Trends Food Sci. Technol. (2021). https://doi.org/10.1016/j.tifs.2021.01.042
13. T.F. Fan, M.G. Potroz, E.L. Tan, M.S. Ibrahim, E. Miyako, N.J. Cho, Sci. Rep. (2019). https://doi.org/10.1038/s41598-019-46131-w
14. E.L. Tan, M.G. Potroz, G. Ferracci, L. Wang, J.A. Jackman, N.J. Cho, Appl. Mater. Today. (2020). https://doi.org/10.1016/J.APMT.2019.100525
15. M. Raish, M.A. Kalam, A. Ahmad, M. Shahid, M.A. Ansari, A. Ahad, R. Ali, Y.A.B. Jardan, A. Alshamsan, M. Alkholief, K.M. Alkharfy, I.A. Abdelrahman, F.I. Al-Jenoobi, Pharmaceutics. (2021). https://doi.org/10.3390/pharmaceutics13111921
16. A.S.Y. Mohammed, A.K.F. Dyab, F. Taha, I Abd El-Mageed RSC Adv. (2022). https://doi.org/10.1039/D2RA02888C
17. N.F. Taha, A.K.F. Dyab, L.H. Emara, N.M. Meligi, J. Drug Deliv Sci. Technol. (2022). https://doi.org/10.1016/j.jddst.2022.103278
18. F.E. Atalay, A.A. Culum, H. Kaya, G. Gokturk, E. Yigit, ACS Appl. Bio Mater. (2022). https://doi.org/10.1021/acsabm.2c00071
19. J. Liu, X.D. Yan, X.Q. Li, Y.H. Du, L.L. Zhu, T.T. Ye, Z.Y. Cao, Z.W. Dong, S.T. Li, X. Xu, W. Bai, D. Li, J.W. Zhang, S.J. Wang, S.H. Li, J. Sun, X.Z. Yin, Front. Immunol. (2023). https://doi.org/10.3389/fimmu.2023.1132129
20. K. Stamatopoulos, V. Kafourou, H.K. Batchelor, S.J. Konteles, Small. (2021). https://doi.org/10.1002/smll.202004573
21. X. Jiang, Y. Liu, H. Hao, Y. Xu, J. Huang, D. Sun, Q. Li, ACS Sustain. Chem. Eng. (2018). https://doi.org/10.1021/acssuschemeng.7b03228
22. J. Kim, J. Deng, N.J. Cho, S.M. Han, Adv. Funct. Mater. (2024). https://doi.org/10.1002/adfm.202313808
23. S. Chen, Q. Shi, T. Jang, M.S. Bin Ibrahim, J. Deng, G. Ferracci, W.S. Tan, N.J. Cho, J. Song, Adv. Funct. Mater. (2021). https://doi.org/10.1002/adfm.202106276
24. K. Hegedüs, C. Fehér, I. Jalsovszky, Z. Kristóf, J. Rohonczy, E. Vass, A. Farkas, T. Csizmadia, G. Friedbacher, P. Hantz, Sci. Rep. (2021). https://doi.org/10.1038/s41598-021-87619-8
25. S.E. Hoover, L.P. Ovinge, J. Econ. Entomol. (2018). https://doi.org/10.1093/jee/toy125
26. J.H. Cane, V.J. Tepedino, Conserv. Lett. (2017). https://doi.org/10.1111/conl.12263
27. Q.Q. Li, K. Wang, M.C. Marcucci, A.C.H.F. Sawaya, L. Hu, X.F. Xue, L.M. Wu, F.L. Hu, J. Funct. Foods. (2018). https://doi.org/10.1016/j.jff.2018.09.008
28. J. Louveaux, A. Maurizio, G. Vorwohl, Bee World. (1978). https://doi.org/10.1080/0005772X.1978.11097714
29. W. Von Der Ohe, L. Persano Oddo, M.L. Piana, M. Morlot, P. Martin, Apidologie. (2004). https://doi.org/10.1051/apido:2004050
30. T.F. Fan, Y. Hwang, M.G. Potroz, K.L. Lau, E.L. Tan, M. Shahrudin Ibrahim, E. Miyako, N.J. Cho, Appl. Mater. Today. (2020). https://doi.org/10.1016/j.apmt.2020.100594
31. AOAC, *Official Methods of Analysis of AOAC INTERNATIONAL*, 20th edn. (AOAC International, Gaithersburg, 2016)
32. A.S. de Carvalho, S.C. de Rezende, C. Caleja, E. Pereira, L. Barros, I. Fernandes, Y.A. Manrique, O.H. Gonçalves, I.C.F.R. Ferreira, M.F. Barreiro, Food Control. (2021). https://doi.org/10.1016/j.foodcont.2021.108262
33. B.P. Binks, A.N. Boa, M.A. Kibble, G. MacKenzie, A. Rocher, Soft Matter. (2011). https://doi.org/10.1039/C0SM01516D
34. P. Aussillous, D. Quéré, Nature. (2001). https://doi.org/10.1038/35082026
35. R. Bleha, T.V. Shevtsova, M. Živčáková, A. Korbářová, M. Ježková, I. Saloň, J. Brindza, A. Synytsya, Foods. (2021). https://doi.org/10.3390/foods10081682
36. Z.M. Portman, M.C. Orr, T. Griswold, J. Hymenopt Res. (2019). https://doi.org/10.3897/jhr.71.32671

37. J.H. Fewell, M.L. Winston, Behav. Ecol. Sociobiol. (1992). https://doi.org/10.1007/BF00176173
38. T.C. Webster, R.W. Thorp, D. Briggs, J. Skinner, T. Parisian, Environ. Entomol. (1985). https://doi.org/10.1093/ee/14.6.683
39. M.J. Uddin, N. Abidi, J. Warzywoda, H.S. Gill, ACS Appl. Mater. Interfaces. (2019). https://doi.org/10.1021/acsami.9b03040
40. J.H. Park, J. Seo, J.A. Jackman, N.J. Cho, Sci. Rep. (2016). https://doi.org/10.1038/srep28017
41. M.J. Uddin, H.S. Gill, J. Control Release. (2017). https://doi.org/10.1016/j.jconrel.2017.10.019
42. S.V. Lale, H.S. Gill, Int. J. Pharm. (2018). https://doi.org/10.1016/j.ijpharm.2018.10.016
43. R.C. Mundargi, M.G. Potroz, J.H. Park, J. Seo, J.H. Lee, N.J. Cho, RSC Adv. (2016). https://doi.org/10.1039/C5RA27207F
44. M.J. Uddin, S. Liyanage, J. Warzywoda, N. Abidi, H.S. Gill, Langmuir. (2022). https://doi.org/10.1021/acs.langmuir.1c02682
45. A. Lutzke, K.J. Morey, J.I. Medford, M.J. Kipper, Phytochemistry. (2020) https://doi.org/10.1016/j.phytochem.2019.112195
46. P. Gonzalez-Cruz, M.J. Uddin, S.U. Atwe, N. Abidi, H.S. Gill, ACS Biomater. Sci. Eng. (2018). https://doi.org/10.1021/acsbiomaterials.8b00304
47. E. Parre, A. Geitmann, Plant. Physiol. (2005). https://doi.org/10.1104/pp.104.050773
48. E. Alpizar-Reyes, J.L. Concha, F.J. Martín-Martínez, J. Norambuena-Contreras, ACS Appl. Mater. Interfaces. (2022). https://doi.org/10.1021/acsami.2c07301
49. C. Pöhlker, J.A. Huffman, U. Pöschl, Atmos. Meas. Tech. (2013). https://doi.org/10.5194/amt-6-3369-2013
50. M.G. Potroz, R.C. Mundargi, J.J. Gillissen, E.L. Tan, S. Meker, J.H. Park, H. Jung, S. Park, D. Cho, S.I. Bang, N.J. Cho, Adv. Funct. Mater. (2017). https://doi.org/10.1002/adfm.201700270
51. M.J. Uddin, S. Liyanage, N. Abidi, H.S. Gill, J. Pharm. Sci. (2018). https://doi.org/10.1016/j.xphs.2018.07.028
52. C. Chiappe, M.J. Rodriguez-Douton, M.C. Mozzati, D. Prete, A. Griesi, L. Guazzelli, M. Gemmi, S. Caporali, N. Calisi, C.S. Pomelli, F. Rossella, Sci. Rep. (2020). https://doi.org/10.1038/s41598-020-68875-6
53. F.S. Li, P. Phyo, J. Jacobowitz, M. Hong, J.K. Weng, Nat. Plants. (2018). https://doi.org/10.1038/s41477-018-0330-7
54. A. Diego-Taboada, T. Sathyapalan, F. Courts, M. Lorch, F. Almutairi, B.P. Burke, K. Harris, M. Kruusmägi, T. Walther, J. Booth, A.N. Boa, S.J. Archibald, C. Thompson, S.L. Atkin, G. Mackenzie, J. Control Release. (2022). https://doi.org/10.1016/j.jconrel.2022.08.017
55. D. Li, L. Sun, L. Shi, L. Zhuo, L. Yang, J. Zhang, Y. Han, T. Ye, S. Wang, Chem. Eng. J. (2023). https://doi.org/10.1016/j.cej.2023.145184
56. S. Bernard, K. Benzerara, O. Beyssac, E. Balan, G.E. Brown, Heliyon (2015). https://doi.org/10.1016/j.heliyon.2015.e00034